

A Magnetic Switch that Determines the Speed of Astrophysical Jets.

Meier, D.L.¹, Edgington, S.^{1,2}, Godon, P.¹, Payne, D. G.³, and Lind, K.R.⁴

1. Jet Propulsion Laboratory, Pasadena, CA, USA.
2. Princeton University, Princeton, NJ, USA.
3. Intel Corporation, Beaverton, OR, USA.
4. Digital Equipment Corporation, Livermore, CA, USA.

Understanding **how** astrophysical **jets** are formed is important for understanding the nature and evolution of such phenomena as active **galactic** nuclei (AGN) and **quasars**, **Galactic** superluminal **X-ray** sources, and young **stellar** objects. Of the many models proposed for jet production, the magnetized accretion **disk** model of Blandford and Payne¹ is the only one that can **operate** in all these regimes and has the **potential** for generating the highly **relativistic flows** seen in some quasars². Here we report on **results** of detailed time-dependent numerical simulations of this mechanism and show that the character and speed of the **jets** produced differ dramatically depending on whether magnetic or **gravitational forces** dominate in the accretion **disk** corona. This “magnetic switch” was not predicted by steady-state, self-similar **disk** models, nor by **relativistic** wind theory (which generally ignores the gravitational **field**). The effect provides a natural explanation, at the black hole accretion **disk** level, for the existence of two known classes of extragalactic radio source (Fanaroff and **Riley** classes I and II) and for the variation of their

properties with radio luminosity. It also provides new insight into protostellar and galactic microquasar systems.

For the past several years we have been studying numerically the flows induced in the coronae of magnetized accretion disks. Our simulations begin with a situation similar to the boundary conditions of Blandford and Payne (BP) and other semi-analytic studies^{3,4} (see figure 1), but are able to investigate time-dependent and two-dimensional effects, unlike the steady-state, self-similar models. A useful parameter for measuring the importance of the magnetic field in the corona is the ratio ν of the speed of magnetic waves in the gas the Alfvén velocity ($V_A \equiv B/[4\pi\rho]^{1/2}$, where B is the magnetic field strength and ρ is the gas density) to the escape velocity ($V_{esc}(r) \equiv [2GM_c/r]^{1/2}$, where M_c is the mass of the central star or blackhole and $r = (R^2 + Z^2)^{1/2}$ is the spherical radial coordinate). In our coronae ν can be rather large, ranging from 0.4 to 2.0 in the simulations we report here. These values are much larger than those investigated by others who have performed similar numerical simulations.⁷⁻¹³

Most of the coronal flows that result in our simulations are decidedly jet-like, but the flow speed and character are strong functions of ν . Figure 2 shows two such cases, each with an initial field polar angle of $\theta = 54^\circ$, but with slightly different values of the Alfvén velocity in the corona. In the low magnetic field case ($\nu = 0.4$), the flow velocity inside the jet is of order the Alfvén speed - $V_{jet} \approx 0.6V_{esc} = 1.5V_A$ (as measured at $R_0 = 7.2r_c$). However, if the Alfvén velocity in the corona is increased by only a factor of three to $\nu = 1.2$ (figure 2b), the jet entirely changes character with a flow speed nearly 20 times that escape speed. We have named these two modes of flow Type 1 and Type 2 jets, respectively, and the transition that occurs from one type to the other the “magnetic switch”.

In addition to the simulations in figure 2, we have performed over 50 others with varying magnetic field strength and polar field angle. Those with $B_p = 0$ in the corona are shown in figure 3, which shows that the magnetic switch is even more dramatic than figure 2 would indicate, with the jet velocity increasing by as much as 80 times when the Alfvén velocity is increased by only 40%. The effect has a simple physical interpretation. When $v < v_A$ (the left-hand side of figure 3), gravitational forces dominate magnetic forces and the jet struggles to escape the system’s gravity. On the right side of the diagram, however, magnetic forces dominate and the system acts like a particle accelerator never really aware of the gravity of the central object.

The behavior of the magnetic switch is not a strong function of the polar magnetic field angle θ ; it exists for all angles studied in figure 3 ($8^\circ - 83^\circ$). In fact, jets still occur for $\theta < 30^\circ$ seemingly contrary to the predictions of BP. The reason is that only in rare cases do the conditions in the disk corona match directly onto the quasi-steady-state jet solutions far above the disk. Instead, there is usually a transition region above the corona where the magnetic poloidal field and flow vectors undergo dramatic changes in direction, and the magnetic field lines *dynamically* acquire an angle greater than 30° . Beyond this transition region, the flow is similar in character to BP’s solutions. Thus, even disks that initially violate BP’s condition for outflow can still form jets, making MHD jet production an even more robust mechanism than previously thought.

Our non-relativistic simulations in figure 3 are applicable to protostellar jets. However, there is some uncertainty in choosing the scale radius r_c and velocity V_c , and hence, the radius $R_0 = 7.2r_c$, where the magnetic field has a maximum and much of the acceleration occurs. If,

for a solar star, $R_0 \approx 200R_{\odot} = 1AU$, then $r_c = 2 \times 10^{12}$ cm and $V_c = 80$ km s $^{-1}$. The magnetic switch then predicts two modes of outflow with a few tens of km s $^{-1}$ for $\nu < 1$ and several hundred km s $^{-1}$ for $\nu > 1$, which is roughly consistent with observations.^{14,15} On the other hand, if the site of acceleration is near the protostar, say $R_0 = 3R_{\odot}$ (many authors have suggested, then the magnetic switch predicts a *low* velocity mode of a few hundred km s $^{-1}$ and a much higher velocity mode with jet velocities of *several thousand* km s $^{-1}$. The latter have not been observed, although a search for such extremely high velocity flow, particularly in the body of known protostellar jets, would be useful. We emphasize that if a hot, tenuous corona (with $\nu > 1$) does not form near the protostar, this high velocity flow will not occur, and the magnetic switch would always be “off”

One class of object in which two modes of jet definitely *have* been observed is the extragalactic radio sources, which are believed to be formed by disk accretion onto black holes¹⁶. Some radio source jets are rather slow ($V_{jet} \lesssim 0.6c$) and dissipate and radiate strongly in the radio shortly after leaving the galaxy nucleus (Fanaroff and Riley class I objects^{17,18}). On the other hand, other radio jets are very fast (Lorentz factor $\gamma \equiv [1 - V^2/c^2]^{-1/2} \lesssim 10$) and do not dissipate or radiate much until they reach large distances from the galaxy and are stopped when the flow strikes the intergalactic medium in a strong shock (FR class II). FRI jets are associated with low power radio sources while FR II with high power, and the transition from FR I to II in radio power is especially sharp if one examines galaxies in a single optical luminosity class¹⁹

Can our non-relativistic simulations be applied to the extragalactic radio source case where relativistic flow and black hole accretion occur? The answer is yes for magnetic field strengths

up to the point where $V_A \sim c$ and, surprisingly, for very high jet speeds ($\gamma \gg 1$). Relativistic effects important here are an increase in mass of the gas due to kinetic and magnetic energies (which limit its velocity to less than c and increase its weight in the black hole's gravitational field) and an electric force perpendicular to the magnetic field lines that affects only their angle²⁰. The velocity terms in the relativistic and non-relativistic flow equations are very similar²¹, involving $(m_{gas} + m_{mag})u$ instead of $m_{gas}v$, where $u = \gamma v$. At every point in the flow we can replace v with γv and, as long as the mass of the magnetic field $m_{mag} \lesssim m_{gas}$ (i.e., $V_A \lesssim c$), our non-relativistic simulations can calculate γ to within a factor of two or so of the actual Lorentz factor. Field angle effects will also be within a factor of two or less in the tangent as long as $V_{esc} \lesssim c$; as we have investigated a range of a factor of 60 in the tangent, and observe the magnetic switch throughout, only the details of the solutions will be affected by the electric force, not our overall conclusions. Finally, the *weight* of the kinetic and magnetic energies will affect only the critical value of the magnetic field $B_{crit} \equiv (4\pi\rho)^{1/2}V_{esc}$ at which the magnetic switch takes place. The condition will still be $\nu = 1$, but we now must use the relativistic value of $V_{esc} = \gamma_0[2(1 - V_A^2/c^2)GM_c/r]^{1/2}$ (for a Schwarzschild black hole, where γ_0 is the jet flow speed while still affected by the black hole's gravity). While γ_0 is probably of order unity, general relativistic MHD simulations will be necessary to confirm this.

Special relativistic calculations of plasma flow in rotating magnetic fields have been performed extensively by many authors in the context of pulsar and jet models. The character and speed of the flow is a function of the magnetization parameter $\sigma = V_A^2 A_0 / (2\pi R_L^2 c V_{i0})$, measured at the place where the outflow originates. (Here $R_L = c/\Omega$ is the radius of the light cylinder, A_0 the disk surface area over which outflow takes place, and V_{i0} is the injection

velocity - equivalent to our injected coronal wind velocity.) The terminal velocity of the flow is given by the simple expression $\gamma_{jet} V_{jet}/c \sim \sigma^n$, where n lies between 2/3 and 1, depending on exactly how the flow collimates^{22,23}. We have plotted these curves in figure 3, with σ on the upper axis, and show that the theory agrees well with our results for $\sigma > \sigma_{crit}$. However, this relation was derived under the assumption that the gravitational force is negligible. Current relativistic wind theory, therefore, is not valid in the region of parameter space where the magnetic switch occurs. Indeed, we can define a critical value of the magnetization ($\sigma_{crit} \equiv V_{esc}^2 A_0 / [2\pi R_L^2 c V_{i0}]$, which is of order unity for the black hole case) below which relativistic wind theory breaks down because gravitational forces become important. For $\sigma < \sigma_{crit}$ ($\nu < 1$) the jet velocity drops rapidly from the $\gamma \gtrsim 10$ result of relativistic wind theory to $V_{jet} \approx 0.1 - 0.4c$.

The magnetic switch occurs in velocity only, not in total jet power. While the jet velocity differs dramatically as the strength of the field is increased through the critical value, we find that the total jet power varies smoothly with the square of the magnetic field, as predicted by Blandford and Payne $P_{jet} \approx B_0^2 R_0^2 (GM_c/R_0)^{1/2}$. For $\nu < 1$, most of the power is in the advected magnetic field, while for $\nu > 1$ the jet carries a significant amount of kinetic power. Both types of power are available for accelerating particles and producing synchrotron radio emission.

The magnetic switch provides a natural explanation for the existence of the FRI and II classes of radio source, with the former being produced by accretion disks with $\nu < 1$ and the latter for $\nu > 1$. Predicted jet speeds agree with observations in each case ($V_{jet} \lesssim 0.6c$ vs. $\gamma \sim 10$ or higher). In addition, the effect explains why the two classes are associated with low

and high power radio sources, respectively, and why the transition is so sharp: both jet power and speed are direct functions of the strength of the magnetic field in the disk corona, but the former is a smooth function while the latter is a strong one. Additional results on variation of the FR I/FR II break with galaxy optical luminosity will be reported elsewhere (Meier 1997, in preparation).

Because the model states that jets in sources with FR I morphology are formed *in the nucleus* with sub-or trans-relativistic velocities, it predicts that, statistically, Very Long Baseline Interferometry observations of FR I sources will show primarily low jet velocities ($V_{jet} < 0.6c$), while FR IIs should have much faster VLBI jets. A corollary is that the parent objects of most BL Lac sources, which have $\gamma = 2 - 5$, cannot have *FR I morphology*.

Finally, bimodal jet ejection has also been observed in the galactic microquasars GRO J1655-40 and Cygnus X-3. Magnetic switching can also explain such behavior, but a detailed determination of the bolometric luminosity of these sources is needed in order to determine whether the triggering mechanism can be a super-Eddington accretion event²⁵ or must be a sub-Eddington event such as a Cygnus X-1 low/high **state** transition.

REFERENCES

- 1 Blandford, R.D. & Payne, D.G. Hydromagnetic flows from accretion discs and the production of radio jets. *Mon. Not. R. Astron. Soc.* **199**, 883-903 (1982).
- 2 Vermeulen, R.C. Superluminal motions: the first 100 sources. In *Extragalactic Radio Sources* (eds Ekers, R., Fanti, C., & Padrielli, L.) 57-62 (IAU Symp. No. 175, Kluwer, Dordrecht, 1996).
- 3 Lovelace, R.V.E., Mehanian, C., Mobarry, C.M., & Sulkanen, M.E. Theory of axisymmetric magnetohydrodynamic flows disks. *Astrophys. J. Supp.* **62**, 1-37 (1986).
- 4 Kudoh, T. & Shibata, H. Mass flux and terminal velocities of magnetically driven jets from accretion disks. *Astrophys. J.* **452**, 1,41-1,14 (1996).
- 5 Shakura, N.I. & Sunyaev, R.A. Black holes in binary systems. Observational appearance. *Astron. Astrophys.* **24**, 337-355 (1973).
- 6 Lind, K.R., Payne, D.G., Meier, D.L., & Blandford, R.D. Numerical simulations of magnetized jets. *Astrophys. J.* **344**, 89-103 (1989).
- 7 Uchida, Y. & Shibata, H. Magnetodynamical acceleration of CO and optical bipolar flows from the region of star formation. *Publ. Astron. Soc. J.* **37**, 515-535 (1985).
- 8 Stone, J.M. & Norman, M.L. Numerical simulations of magnetic accretion disks. *Astrophys. J.* **433**, 746-756 (1994).
- 9 Bell, A.R. & Lucek, S.G. Magnetohydrodynamic jet formation. *Mon. Not. R. Astron. Soc.* **277**, 1327-1340 (1995).
- 10 Matsumoto, R. Three-dimensional global MHD simulations of magnetised accretion disks

and jets. In *Accretion Phenomena and Related Outflows* (IAU Colloq. No. 163) in press (1996).

11 Koide, S., Shibata, K., & Kudoh, T. General relativistic simulation of jet formation from a magnetized accretion disk. In *Accretion Phenomena and Related Outflows* (IAU Colloq. No. 163) in press. (1996).

12 Ustyugova, G.V., Koldoba, M.M., Romanova, V.M., Chechetkin, V. M., & Lovelace, R. V. E. Magnetohydrodynamic simulations of outflows from accretion disks. *Astrophys. J.* 439, L39-L42 (1995).

13 Ouyed, R., Pudritz, R.E., & Stone, J. M. Episodic jets from black holes and protostars. *Nature* 385, 409-414 (1997).

14 Bachiller, R. Bipolar molecular outflows from young stars and protostars. *Ann. Rev. Astron. Astrophys.* 34, 111-154 (1996).

15 Eislöffel, J. Observational properties of jets from young stars. In *Jets from Stars and Galactic Nuclei* (ed Kundt, W.) 101-117 (Lecture Notes in Physics, Vol. 471, Springer, Berlin, 1996).

16 Blandford, R.D. & Rees, M.J. The standard model and some new directions. In *Testing the AGN Paradigm* (eds Holt, S. S., Neff, S.G. & Urry, C.M.) 3-19 (AIP Conf. Proc. 251, Am. Inst. Phys. College Park, MD, 1991).

17 Fanaroff, B.L., and Riley, J.M. The morphology of extragalactic radio sources of high and low luminosity. *Mon. Not. R. Astron. Soc.* **167**, 311-351 (1974).

18 Bicknell, G.V. The relationship of the Fanaroff-Riley classification of extragalactic radio-

sources to jet physics. *Publ. Astr. Soc. Aus.* **6**, 130-137 (1985)

19 Ledlow, M.J. & Owen, F.N. 20-cm VLA survey of Abell clusters of galaxies. VI. Radio/optical luminosity functions. *Astron. J.* **112**, 9-22 (1996).

20 Li, Z.-Y., Chiueh, T., & Begelman, M.C. Electromagnetically driven relativistic jets: a class of self-similar solutions. *Astrophys. J.* **394**, 459-471 (1992).

21 Goldreich, P. & Julian, W.H. Stellar winds. *Astrophys. J.* **160**, 971-977 (1970)

22 Henriksen, R.N. Jets and magnetic fields. In *Accretion Disks and Magnetic Fields in Astrophysics* (ed Bekevedere, G.) 117-128 (Kluwer, Dordrecht, 1989).

23 Camenzind, M. Hydromagnetic flows from rapidly rotating compact objects and the formation of relativistic jets. In *Accretion Disks and Magnetic Fields in Astrophysics* (ed Bekevedere, G.) 129-143 (Kluwer, Dordrecht, 1989).

24 Hjellming, R.M. Imaging relativistic radio jets and the X-ray- radio connection in X-ray transients. In *Accretion Phenomena and Related Outflows* (IAU Colloq. No. 163) in press. (1996).

25 Meier, D.L. A super-Eddington wind model for GRO J1655-40. In *Accretion Phenomena and Related Outflows* (IAU Colloq. No. 163) in press. (1996).

ACKNOWLEDGEMENTS. Part of this research was carried out at the Jet Propulsion Laboratory, under contract to NASA. S.E. acknowledges the support of an Associated Western Universities Summer Fellowship. During this research, P.G. held a National Research Council Research Associateship at the NASA Jet Propulsion Laboratory. We are grateful to R. Linfield,

R. Ouyed, R. Hjellming, and K. Meisenheimer for helpful comments on the manuscript.
CORRESPONDENCE should be addressed to D.L.M. (e-mail: dlim@cena.jpl.nasa.gov).

FIGURE 1

Schematic representation of the initial and boundary conditions for our accretion disk corona simulations. A dense accretion disk (dark material) orbits a compact object (star or black hole) of mass M_c and scale radius r_c , which is also our unit of distance and our mesh spacing. (We take $r_c = 2 \times 10^{12}$ cm and GM_c/c^2 for the protostar and black hole cases, respectively, so the radius at which much of the acceleration takes place [$R_0 = 7.2r_c$] is $\sim 1M$ and ~ 3.6 Schwarzschild radii. See text **for** more discussion.) Open magnetic field lines, making an angle θ with the rotation axis, protrude from the disk and through a much less dense and more extended corona whose temperature is hotter than the disk but still colder than the (virial) temperature of a halo that permeates the rest of the system. The coronal density is assumed to be ten (10) times the asymptotic halo density; the disk density is many orders of magnitude larger than that essentially infinite in our simulations. The corona is replenished continually from below with a wind of the same material at a velocity of only 5% of the escape speed at that point in the disk ($V_{esc} = [2GM_c/R]^{1/2}$). The sound speed in this wind is only 0.9% of the local escape speed truly cold disk material but, because of shock heating, the wind velocity is more representative of the eventual coronal sound speed. At their base the field lines are poloidal only ($B_\phi = 0$) and are anchored in the dense disk, rotating with the local Keplerian angular velocity ($\Omega_K = [GM_c/R^3]^{-1/2}$) but having no appreciable radial motion. This assumption is valid for time scales short compared with the accretion drift time (~ 5 months for a $10^8 M_\odot$ AGN black hole, ~ 1 second for a $10 M_\odot$ Galactic black hole, and ~ 2 months for a $1 M_\odot$ protostar) and when the magnetic field is not strong enough to disrupt the disk itself ($V_A^{disk} \ll V_{esc}$). Standard accretion **disk** models like the α -model⁵ naturally

have a low Alfvén velocity. However, if a low-density corona also exists, V_A there can be much higher for the same magnetic field line by the ratio $(\rho_{disk}/\rho_{corona})^{1/2}$. A large number of accretion disks, therefore, can possess fairly benign magnetic fields that are still strong enough to appreciably affect the dynamics of their coronae ($V_A^{corona} \gtrsim V_{esc}$). Our simulations are allowed to evolve from these initial conditions, using our axisymmetric magnetohydrodynamic (MHD) simulation code FLOW⁶. The simulation region is bounded at $Z = 0$ by the infinitely thin disk and inflow region for $5r_c \leq R \leq R_{max}$ and reflective conditions for $0 < R < 5r_c$; by the rotation axis at $R = 0$; and by open (“outflow”) boundaries at $R = R_{max}$ and $Z = Z_{max}$.

FIGURE 2

logarithmic gray-scale plots of magnetic pressure ($B^2/8\pi$) for two MHD disk corona simulations that differ in only one respect: the disk coronal magnetic field strength in **b** is a factor of three (3) larger than that in **a**. The disk in figure 1 lies along the left ($Z = 0$) axis. Both have a field polar angle of 54° , and we show both when the jet reaches the maximum extent of the mesh. The simulation in panel **a** has a ratio of Alfvén to escape velocity of $\nu = 0.1$ throughout the disk corona and is shown after ~ 8.6 disk rotation times (as measured at $R = R_0$). Even though the simulation begins with gravitational forces dominating, the azimuthal component of the magnetic field increases in strength due to differential rotation, recoils upward and is able to eject a slow jet with a speed of $0.6V_{esc}(R_0)$. This is also approximately the propagation speed of the jethead through the external medium, indicating that the jet is fairly heavy. The simulation in panel **b** has $\nu = 1.2$ and is displayed at ~ 4.5 rotation times. This jet is produced by magneto-centrifugal acceleration, rather than magnetic recoil, but still has a significant

enough azimuthal field for collimation. Its internal speed is $19V_{esc}(R_0)$ over 30 times faster than the jet in **a** and ~ 20 times faster than propagation of the jet head, indicating that this jet is very light ($\rho_{jet} \ll \rho_{halo}$).

FIGURE 3

Jet speed as a function of coronal magnetic field strength and angle for both stellar accretion disks (lower and left axes) and black hole disks (upper and right axes). The **stellar** interpretation of our multi-simulation results shows V_{jet}/V_c vs. magnetic field strength in terms of $V_A(R_0)/V_c$, where V_c is the *Kepler velocity* at r_c ($[GM_c/r_c]^{1/2}$). We also show simulation results from references [12] and [13]. While differing from ours in some respects, **most** notably in having significant gas pressure and non-zero $B_{\phi 0}$ (both of which we have found tend to increase the jet velocity), their results still agree roughly with ours in the $\nu < 1$ region. The different curves show families with the same polar magnetic field angle θ : \triangle 8° ; \square 24° ; \circ 35° ; A 54° ; \blacklozenge 68° ; \bullet 83° . For small angles, the speed and power of the jet diminishes at the expense of a loosely- or un-collimated magnetic wind emanating from a large part of the disk outside the jet-production region. This wind also displays the magnetic switch effect.

The black hole interpretation shows the product of the jet velocity and Lorentz factor ($\gamma_{jet}\beta_{jet} \equiv V_{jet}/[c^2 - V_{jet}^2]^{1/2}$) vs. the magnetization parameter at $R_0 = 7.2GM_c/c^2$ (using $\Omega = \Omega_K$, $V_{i0} = 0.05V_{esc}$, $V_c = c$, and an injection region of $\Delta r \sim 2R_0$): $\sigma = V_A^2 V_{esc}^2 / (c^3 V_{i0}) = 11(V_A/V_c)^2$. We also plot the well-known result from relativistic wind theory^{22,23} $(\gamma\beta)_{jet} = \sigma^n$ for $n=2/3$ and $n=1$, which is valid only for $\sigma > \sigma_{crit} \approx 11(V_{esc}/c)^2 = 3.1$ for the black hole case. our simulations agree with relativistic wind theory in this regime to within the factor of

two or so error estimated in the text. For truly *general* relativistic MHD simulations, the value of σ_{crit} , and the curves, will be shifted to the right by a factor of $\sim \gamma_0[1+(V_{esc}/c)^2]^{1/2} = 1.13\gamma_0$. While γ_0 could be as high as γ_{jet} , it is most likely of order unity (smooth acceleration over a few R_0 in distance).

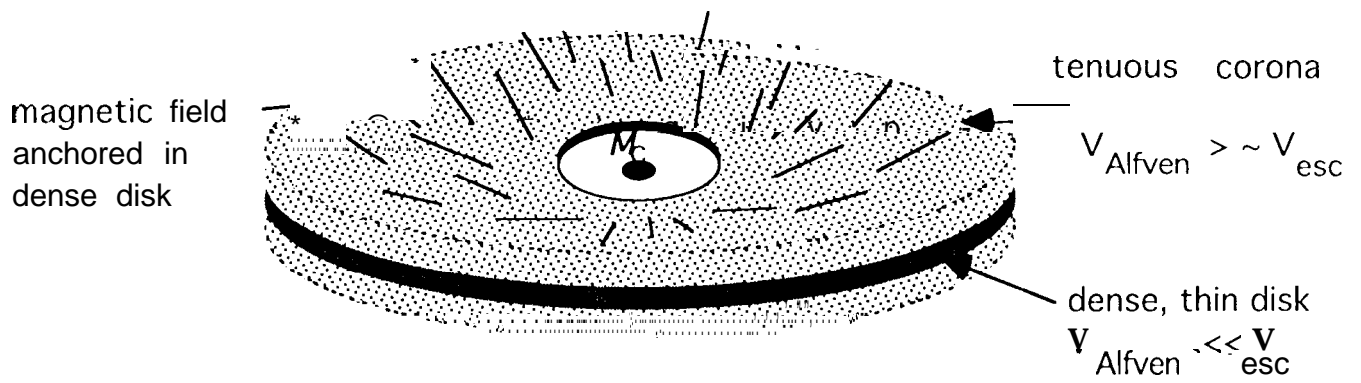


FIGURE 1

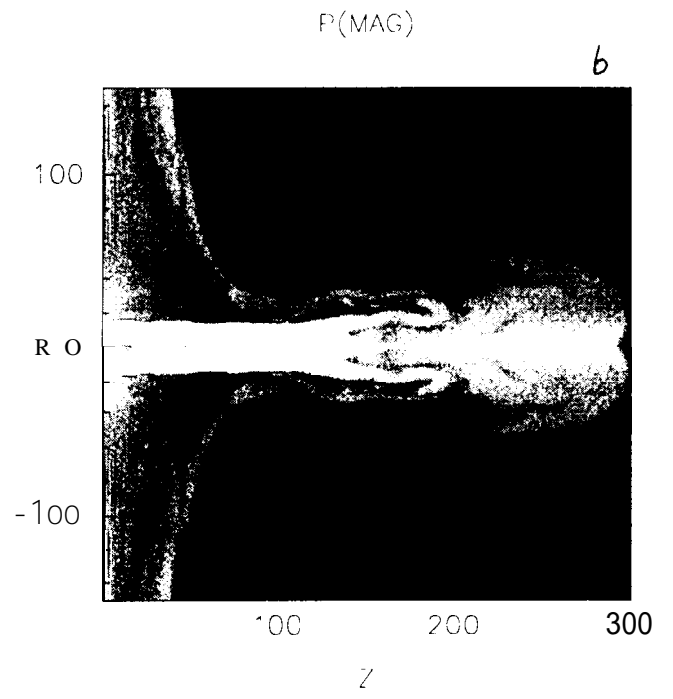
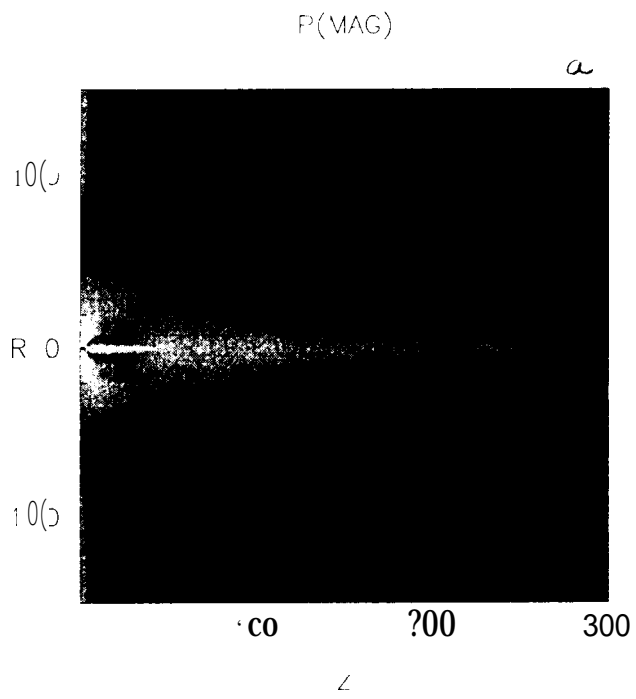


FIGURE 2

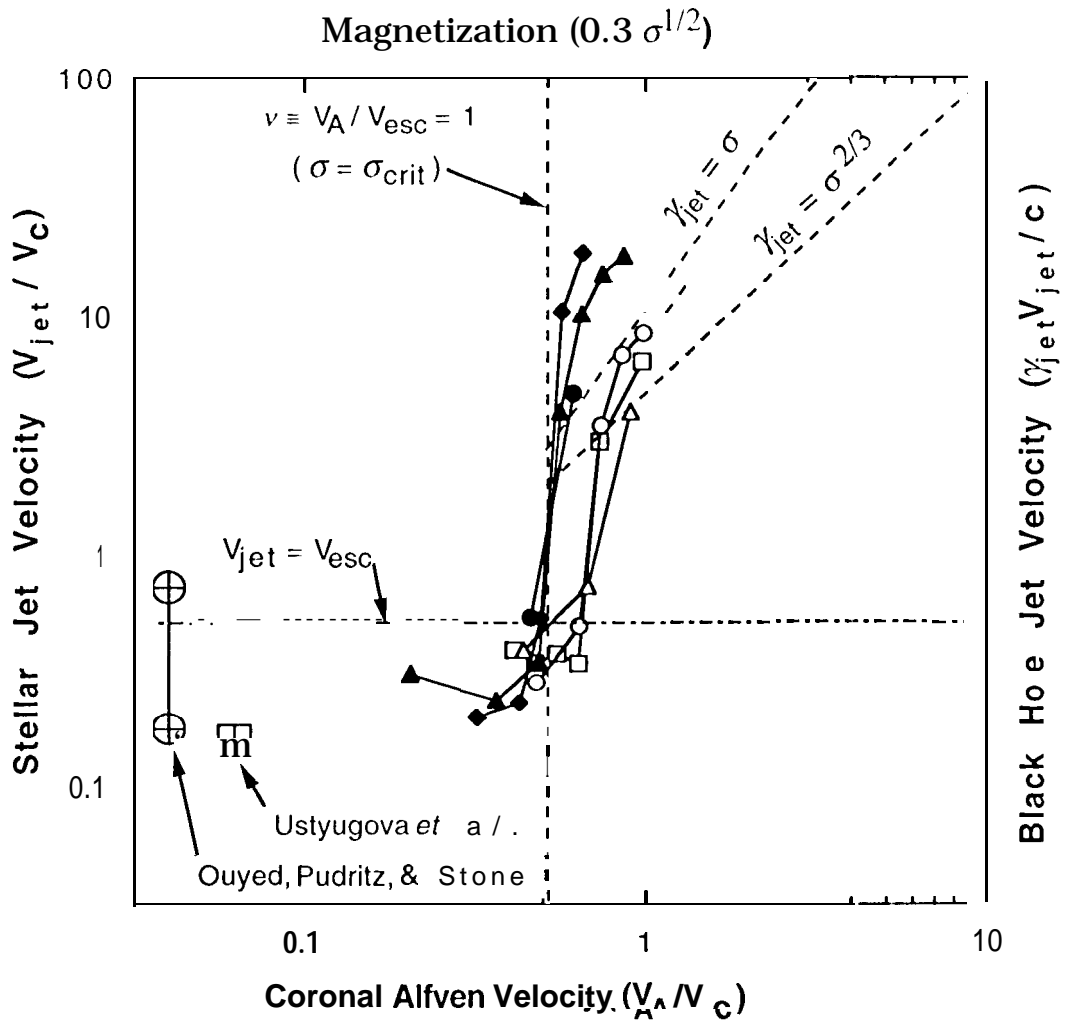


FIGURE 3